

MOLECULES AT EARLY EPOCHS. IV. CONFIRMATION OF THE DETECTION OF H₂ TOWARD PKS 0528 – 250¹

CRAIG B. FOLTZ AND FREDERIC H. CHAFFEE, JR.

Multiple Mirror Telescope Observatory; Smithsonian Institution, and the University of Arizona

AND

JOHN H. BLACK

Steward Observatory, University of Arizona

Received 1987 March 24; accepted 1987 June 23

ABSTRACT

We present new spectroscopic observations of the QSO PKS 0528–250 obtained with 1 and 5 Å resolution. The observed wavelengths of the C iv $\lambda\lambda$ 1548, 1550 and Si iv $\lambda\lambda$ 1393, 1402 emission lines yield a reliable determination of the redshift of $z_{em} = 2.770 \pm 0.005$. We examine the absorption system at $z_{abs} = 2.811$ for absorption by molecular hydrogen and find strong evidence supporting the claim by Levshakov and Varshalovich of its existence in this system. While it is difficult to assess the statistical reality of this identification, we argue that it is fairly secure. Given the identification, a limited search of parameter space yields the following column density, Doppler parameter, and excitation temperature: $N(\text{H}_2) = 10^{18} \text{ cm}^{-2}$, $b = 5 \text{ km s}^{-1}$, and $T_{ex} = 100 \text{ K}$. The identity of the redshift of features from bands with increasing vibrational quantum number of the upper state allows us to set a limit on the fractional change of the ratio of the electron to proton inertial mass over the interval of cosmic time from $z = 2.811$ to the present of less than 2×10^{-4} . We also discuss the implications of the detection for our understanding of the physical processes in the absorbing cloud and suggest topics for further study.

Subject headings: galaxies: intergalactic medium — quasars

I. INTRODUCTION

In the series of papers of which this is a part (Chaffee, Foltz, and Black 1986; hereafter Paper I, Black, Chaffee, and Foltz 1987, hereafter Paper II; Chaffee, Foltz, and Black 1988, hereafter Paper III) we have attempted to confirm some of the earlier claims of the detection of molecular transitions in absorbing clouds toward high-redshift QSOs. In all cases we were unable to confirm previous claims, only to set upper limits on the column densities of molecular species. Discussions of earlier claims for the detection of molecular absorption can be found in Papers I–III.

In Papers II and III, we concentrated our attention on systems with sufficiently high H I column density to produce strong Ly α absorption. This class of system is easily identified on the basis of the damped Ly α absorption profile. A catalog of these “Ly α disk” systems was recently published by Wolfe *et al.* (1986). In Paper II, we presented new high-resolution, high signal to noise (S/N) observations of perhaps the best-known Ly α disk system: the $z = 2.309$ system toward PHL 957. This system has had the most claims made for the possible detection of absorption by H₂ due to coincidences between the wavelengths of H₂ lines predicted to be strong and observed lines in the Ly α forest of PHL 957. By searching for *anticoincidences* between the observed spectrum and synthetic H₂ spectra for a range of excitation temperature and by searching for transitions of CO longward of the Ly α forest, we were able to set limits of 2×10^{-8} and 4×10^{-6} for $N(\text{CO})/N(\text{H})$ and

$2N(\text{H}_2)/N(\text{H})$, respectively, that are lower than corresponding Galactic values by factors of 10 and 1.25×10^5 .

In Paper III we studied the $z = 1.776$ system toward the QSO MC 1331 + 170. In this case, the redshift of the system is low enough that the Lyman and Werner bands of H₂ are below the atmospheric cutoff so we were able to set limits only on $N(\text{CO})/N(\text{H})$.

A well-known Ly α disk system which does not appear in the catalog of Wolfe *et al.* is the system at $z_{abs} = 2.811$ toward the QSO PKS 0528 – 250. This system was studied at low spectral resolution by Smith, Jura, and Margon (1979) and subsequently at 2 Å resolution by Morton *et al.* (1980) and Chen and Morton (1984). The column density of this system in neutral hydrogen is comparable those in the systems in PHL 957 and MC 1331 + 170 and the redshift of the system is higher so that the lines of H₂ at rest wavelengths between ~ 930 Å and 1110 Å are redshifted to wavelengths that are easily observed with terrestrial telescopes, even at 31° north latitude.

Additional stimulation to observe this system was provided by the reported detection of H₂ by Levshakov and Varshalovich (1985) in this system based on the spectrum published by Morton *et al.* In light of the spurious nature of all previous such claims, we were skeptical of the identifications and expected that higher S/N and higher resolution observations would turn up a number of *anticoincidences* between the observed and predicted spectra for any reasonable H₂ column density and excitation temperature. To this end, we obtained higher quality spectra than were previously available. Contrary to our expectations, however, upon investigation of these data, we found that the observations are consistent with an H₂ column density of $\sim 10^{18} \text{ cm}^{-2}$, and this paper reports our evidence supporting that detection.

¹ Observations presented here were obtained with the Multiple Mirror Telescope, a facility operated jointly by the Smithsonian Institution and the University of Arizona.

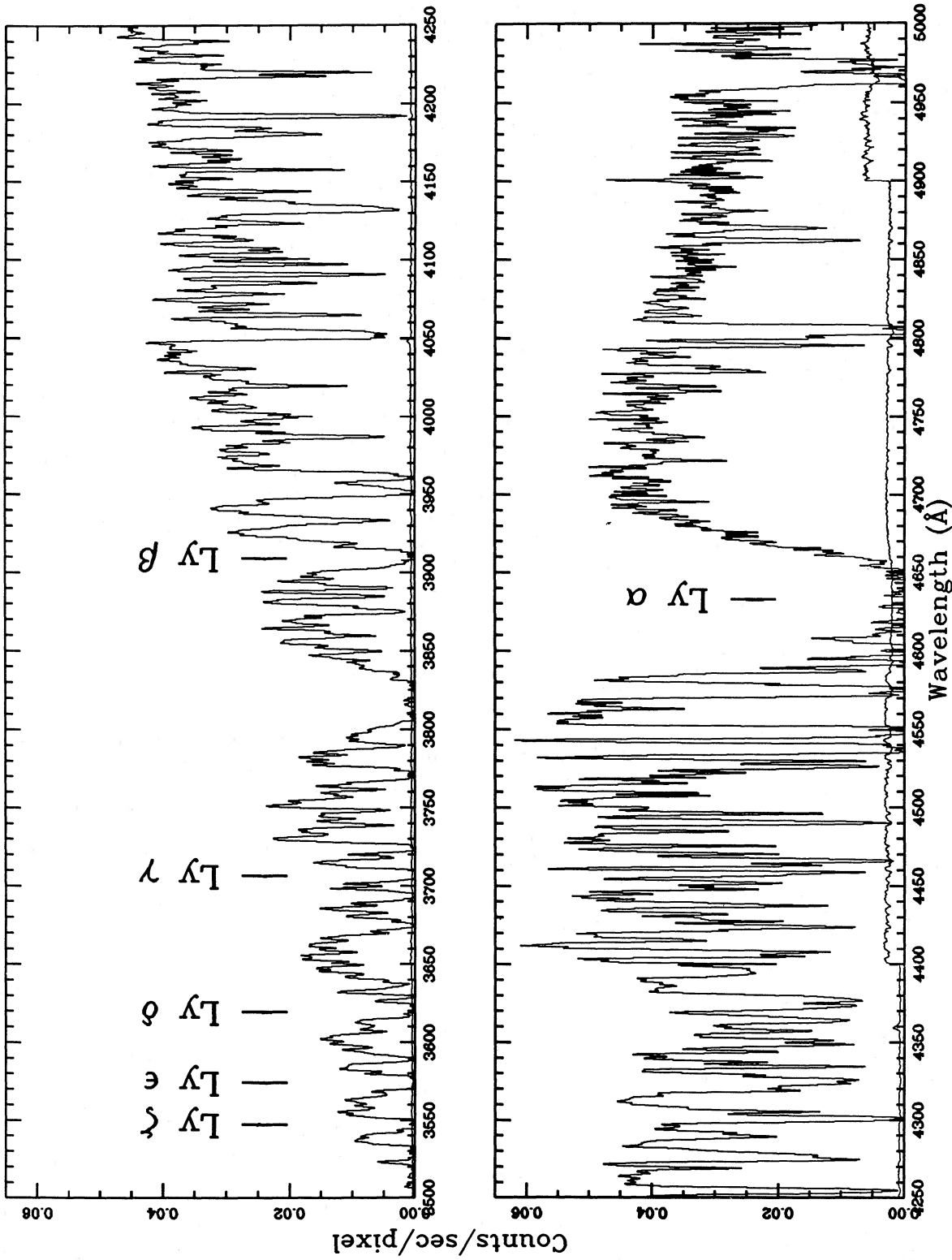


FIG. 1.—Composite of all of the 1 Å resolution data of PKS 0528-250. The positions of the Lyman absorption lines in the $z = 2.8110$ system are marked. The lower spectrum in this and subsequent figures is the rms noise level as derived from consideration of counting statistics in the object, sky, and dark signals. Discontinuities in the “error spectrum” indicate wavelengths where individual scans overlap. The data intensity scale has not been corrected for atmospheric extinction or the wavelength-dependent sensitivity of the instrument.

TABLE 1
PKS 0528–250: JOURNAL OF OBSERVATIONS

Date (UT)	Wavelength Range (Å)	Integration Time (s)	Resolution FWHM (Å)
1986 Oct 26	3200–4100	7200	1
1986 Nov 1	4100–5000	600	1
1986 Dec 1	3500–4400	4800	1
1986 Dec 1	4100–5000	4800	1
1986 Dec 24	3500–4400	6000	1
1986 Dec 29	3500–4400	6600	1
1987 Feb 6	3200–7200	3600	5
1987 Feb 23	3200–7200	4800	5
Total		38400	...

II. OBSERVATIONS

All observations reported here were made with the Multiple Mirror Telescope and MMT Spectrograph. A summary of observations is presented in Table 1. PKS 0528–250 was observed at two spectral resolutions: our 1 Å resolution (FWHM) data span the wavelength range from 3200 to 5000 Å, and the 5 Å resolution spectra cover the range from 3200 to 7200 Å. In reality, the confluence of Lyman lines shortward of $\text{Ly}\theta$ and the Lyman continuum of the $z = 2.811$ system obliterate the flux shortward of 3500 Å. All observations were made using the “image stacker” (Chaffee and Latham 1982) which yields the above mentioned spectral resolution with 2/5 diameter entrance apertures.

Our data reduction procedures are described in Papers I and II and will not be discussed here except to note that the high-resolution spectra were corrected for neither atmospheric extinction nor the wavelength-dependent sensitivity of the instrument while the low-resolution data were corrected for these effects using mean extinction coefficients appropriate for

Mount Hopkins and observations of the standard star EG 42 (Oke 1974). The latter observations were obtained during conditions of good seeing but variable transparency, resulting in an unknown scale error in the absolute flux calibration.

The 1 Å data are presented in Figure 1. We have marked the positions of Lyman lines in the $z = 2.811$ system. The low-resolution data are presented in Figure 2. In both Figures, the lower curve is the 1σ error spectrum obtained by properly accounting for, and weighting by, the variance of each datum as derived from counting statistics in the object, sky, and dark signals.

III. INTERPRETATION

a) The Emission-Line Redshift

PKS 0528–250 is somewhat unique in that it does not show strong $\text{Ly}\alpha$ emission. In part, this may be due to the overall weakness of the emission line spectrum and, in part, to the presence of the damped $\text{Ly}\alpha$ absorption. Emission lines of C IV and Si IV are clearly present in the spectrum in Figure 2. These lines have a heliocentric, vacuum redshift of $z_{\text{em}} = 2.770 \pm 0.005$, in substantial agreement with estimates in earlier investigations (Smith, Jura, and Margon 1979: $z_{\text{em}} = 2.765 \pm 0.010$; Chen and Morton: $z_{\text{em}} = 2.767 \pm 0.002$). With adoption of 2.77 as the emission line redshift and 2.8110 for the absorption lines, the absorption line system lies $3250 \pm 400 \text{ km s}^{-1}$ longward of the emission line redshift. As noted by Smith, Jura, and Margon, this value is considerably larger than the velocity dispersion of a typical cluster of galaxies. However, the well-known tendency for high-ionization broad lines to have centroids which lie systematically shortward of the systemic redshift (see, for example, Gaskell 1982 and Wilkes and Carswell 1982) by up to several thousand km s^{-1} may ameliorate the discrepancy.

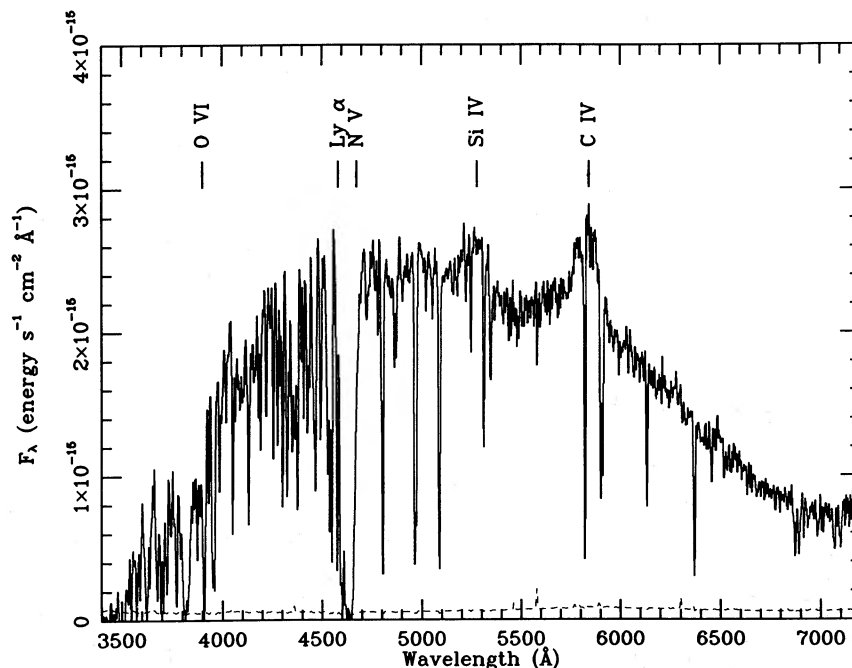


FIG. 2.—Sum of the 5 Å resolution data showing the presence of strong C IV $\lambda 1550$ and Si IV $\lambda 1400$ emission at a redshift of 2.770 ± 0.005 . The expected positions of other strong emission lines at this redshift are also shown.

b) The H I Lines

We have fitted a continuum level to the data in Figure 1 by eye. The errors in this procedure are difficult to estimate, and they propagate through the rest of our analysis in an unknown way. However, given the extreme line blending in the Ly α forest at this redshift, we were not able to devise an objective method of determining the continuum level. The data in Figure 1 were then converted to residual intensity by dividing by this continuum. The resulting spectrum is presented in Figure 3.

Synthetic spectra of Voigt profiles with various values of z_{abs} , $N(\text{H I})$, and Doppler parameter, b , were generated for Ly α through Ly ϵ and were fitted to the normalized data. The goodness of fit was judged by eye. In practice, $N(\text{H I})$ was constrained fairly tightly by the Ly α profile, z was constrained by the positions of the extremes of the saturated cores of

Ly β through Ly ζ , and b was constrained by the wavelength of the Lyman discontinuity. A reasonable fit to the observed Lyman series is obtained for the following parameters: $\log N(\text{H I}) = 21.1 \pm 0.3$, $z = 2.8110 \pm 0.0003$, and $b = 100 \text{ km s}^{-1}$.

The redshift of the Lyman series is identical to that of system A₂ in the nomenclature of Morton *et al.* and Chen and Morton. Presumably the large Doppler parameter does not result from thermal motion, but rather from multiple components at small velocity spacings. There are no resolved sub-components in any of the Lyman lines, but low ionization lines of Fe, Si, and O in system A in the above mentioned studies are clearly double with a component at $z_{\text{A}1} = 2.81322$ and $z_{\text{A}2} = 2.81100$. While we could probably have fitted the Lyman series data with two components at these redshifts, we find that they are consistent with a single component. We note that the

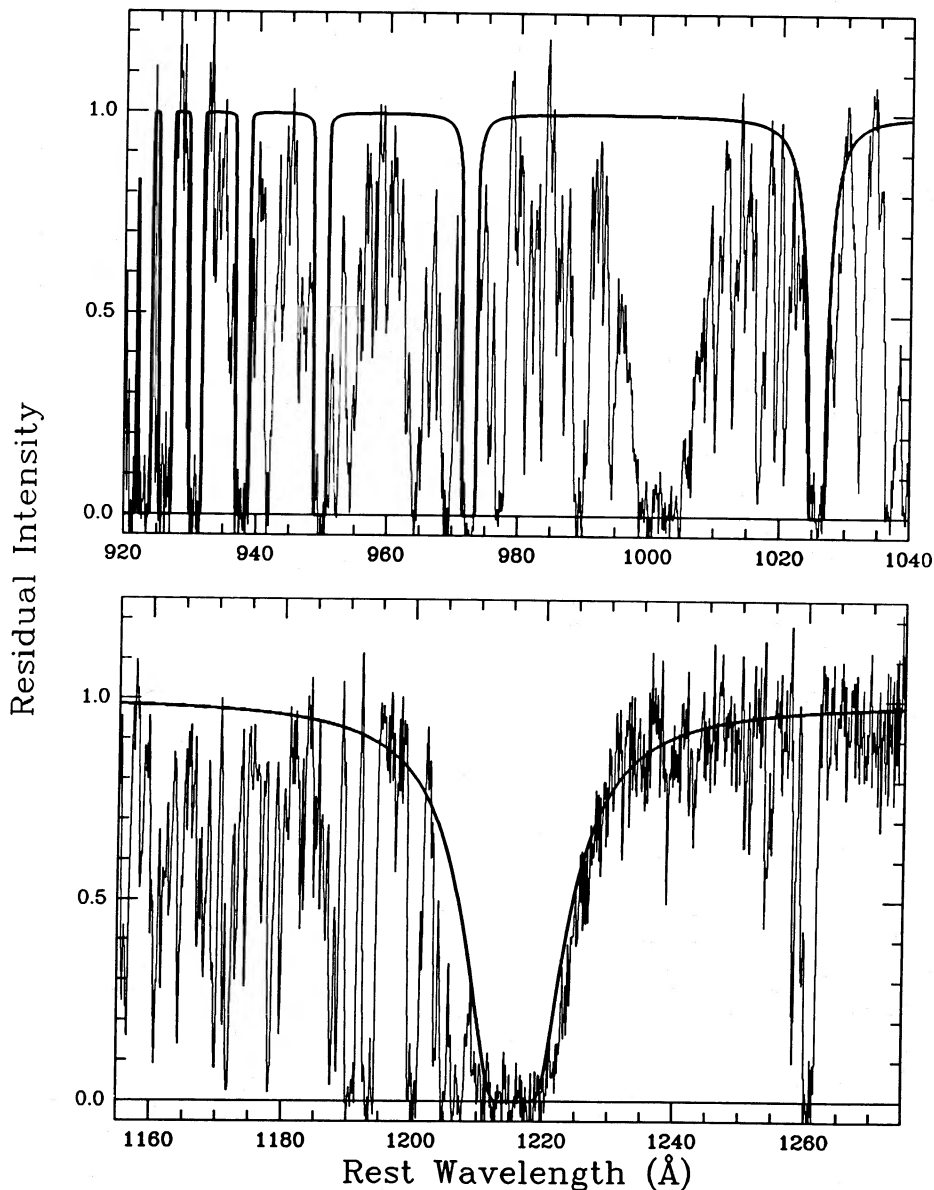


FIG. 3.—Comparison of the 1 Å resolution data (divided by a continuum level which was fitted by eye) with synthesized atomic hydrogen Lyman absorption lines. The Lyman lines are appropriate for an absorbing cloud with the following parameters: $z = 2.8110$, $N(\text{H I}) = 1.25 \times 10^{21} \text{ cm}^{-2}$, $b = 100 \text{ km s}^{-1}$.

column density is no larger than that found for the damped systems in both PHL 957 [Paper II; $\log N(\text{H I}) = 21.4$] and MC 1331 + 170 [Paper III; $\log N(\text{H I}) = 21.2$].

c) The H_2 Lines

i) Evidence for H_2 Absorption

In Figure 4 we plot the normalized data in the regions where strong H_2 absorption lines in the $z = 2.811$ system are expected. Superposed on the data is a synthetic spectrum H I Lyman lines and H_2 lines of the Lyman and Werner bands. The synthetic spectrum contains 396 lines of H_2 with rotational quantum number $J \leq 7$ in the Lyman 0–0 through 20–0 and Werner 0–0 through 6–0 bands that have rest wavelengths $\lambda \geq 911.7 \text{ \AA}$. The H I lines were generated using the following parameters: $\log N(\text{H I}) = 21.1$, $z_{\text{H I}} = 2.8110$, $b_{\text{H I}} = 100 \text{ km s}^{-1}$; the H_2 lines are appropriate for $\log N(\text{H}_2) = 18$, $z_{\text{H}_2} = 2.8108$, and $b_{\text{H}_2} = 5 \text{ km s}^{-1}$ (see below for a discussion of how these were derived). There is a remarkable agreement between the two spectra in the sense that while a large number of the H_2 lines are coincident with the positions of strong Lyman α forest lines at different redshifts, a number of H_2 lines are coincident in wavelength and in strength with weak features. Furthermore, there are no strong anticoincidences. The strongest discrepancy, in the sense that the synthetic spectrum predicts absorption which is stronger than is seen in the real data is $\sim 933 \text{ \AA}$, a region of low S/N and uncertain placement. We feel that the general agreement is compelling and discuss the properties of the H_2 lines below. Because of the uncertainties in the establishment of the continuum, it is difficult to assess the statistical reality of weak features in the Ly α forest. Furthermore, since much of the H_2 absorption is at wavelengths where it can be confused not only with intervening Ly α absorption in Ly α forest systems at lower redshifts, but also with higher Lyman lines in such systems, we cannot even estimate the probability of observing such a large number of wavelength coincidences with no anticoincidences by Monte Carlo simulation. To perform such a calculation we would require a knowledge of both the number per unit redshift and column density distributions of Ly α forest systems at this redshift. We consider the errors in both to be sufficient to vitiate such simulations.

We feel, however, that the probability of the observed configuration of lines occurring by chance is very small. In order to demonstrate this, in Figure 5a, we replot the synthetic H_2 spectrum from Figure 4, omitting the H I lines and displaying the spectrum on a logarithmic wavelength scale. The normalized PKS 0528–250 1 \AA data are plotted on an identical scale in Figure 5b. The reality of the H_2 identification can best be seen by reproducing Figure 5a onto a transparency and overlaying it onto Figure 5b. Horizontal shifts of these two plots with respect to one another are equivalent to Doppler shifts and vertical shifts to errors in continuum placement. By performing this exercise it is easily seen that: (1) A small relative shift between the two spectra (or order one line width or more) can result in the introduction of a large number of anticoincidences. (2) The lines which we identify as H_2 do not show conspicuous structure. That is, there is no other component at small velocity offset of comparable strength to that we tentatively identify as H_2 in the $z = 2.811$ system.

A more quantitative test of the identification carried out by crosscorrelating Figures 5a and 5b. This was accomplished using the software developed by Tonry and Davis (1979). The cross-correlation function was computed for lags in the range

$-10,000 \leq \Delta v \leq 10,000 \text{ km s}^{-1}$ and strong H I lines were excised from the data before the correlation was carried out. The central $12,000 \text{ km s}^{-1}$ of the cross-correlation function is presented in Figure 6. Note the strong peak near zero velocity shift. We could not determine the significance of the peak but do note that its peak amplitude is more than a factor of 2 higher than that of any other peak within the full range of the calculation. The S/N of the cross correlation is far worse than the S/N of the observed spectrum, of course, because the spectrum is so rich in features at a variety of redshifts that cannot be included in a simulated template spectrum *a priori*. We also carried out correlations of the synthetic H_2 spectrum against the mirror image of the observed data and against a spectrum constructed by interchanging the first and second halves of the observed spectrum. In no case did a peak of more than about one-half the strength of the central peak in Figure 6 result. Finally, we note that peaks with amplitude similar to that seen near -4000 km s^{-1} in Figure 6 are seen in the autocorrelation of the H_2 spectrum. If the identification of H_2 is correct, the cross correlation of the synthetic and real spectra will contain some of the features in the H_2 autocorrelation so that peaks of this amplitude may *not* be due solely to noise induced by the confusing Ly α forest lines.

In summary, the data presented here are reasonably compelling support for the identification of H_2 in the spectrum of PKS 0528–250 by Levshakov and Varshalovich (1985).

ii) Redshift of the H_2 Absorption

The large b -value derived from profile fitting to the H I lines and the obvious structure in the low-ionization atomic lines imply that there is considerable structure in the H I velocity distributions which in turn implies considerable structure in the H I spatial distribution. As noted above, the H_2 lines apparently exhibit only one component. In order to derive the H_2 redshift, the rest frame into which the observed spectrum was transformed was varied until a best-fit (as judged by eye) with the coincident features in the synthetic spectrum was obtained. We subsequently identified 26 features in the spectra which agreed well in both wavelength and strength and, therefore, stood the best chance of being due to H_2 absorption. Since these features could potentially be blends even in the synthetic spectrum, we measured the wavelengths of the features in both the synthetic and real spectra. These are tabulated in Table 2 along with the redshift of the observed feature and the identification of the transitions making up the feature. The mean redshift derived from these lines is $z_{\text{H}_2} = 2.81086 \pm 0.00020$. The error quoted is the standard deviation of the mean redshift of all 26 features, unweighted for blending and is larger than the error of 0.00005 in a single redshift measurement which results from the typical uncertainty in the wavelength calibration. The H_2 redshift is indistinguishable from the H I redshift of 2.8110 ± 0.0003 and is consistent with the H_2 absorption being in system A2 as defined by Chen and Morton ($z_{\text{A}2} = 2.81100$) and certainly not in system A1 ($z_{\text{A}1} = 2.81322$). The lines listed in Table 2 have no plausible alternative identifications with atomic lines at $z = 2.811$, except as indicated in the notes to the table.

iii) H_2 Column Density, Doppler Parameter, and Temperature

The spectrum of molecular hydrogen is determined by the H_2 column density, its Doppler parameter, and its excitation temperature, T_{ex} . We chose not to attempt to find the “best-fit” values of $N(\text{H}_2)$ and T_{ex} via a procedure which minimizes χ^2 for the following reasons: (1) The dominant source of error

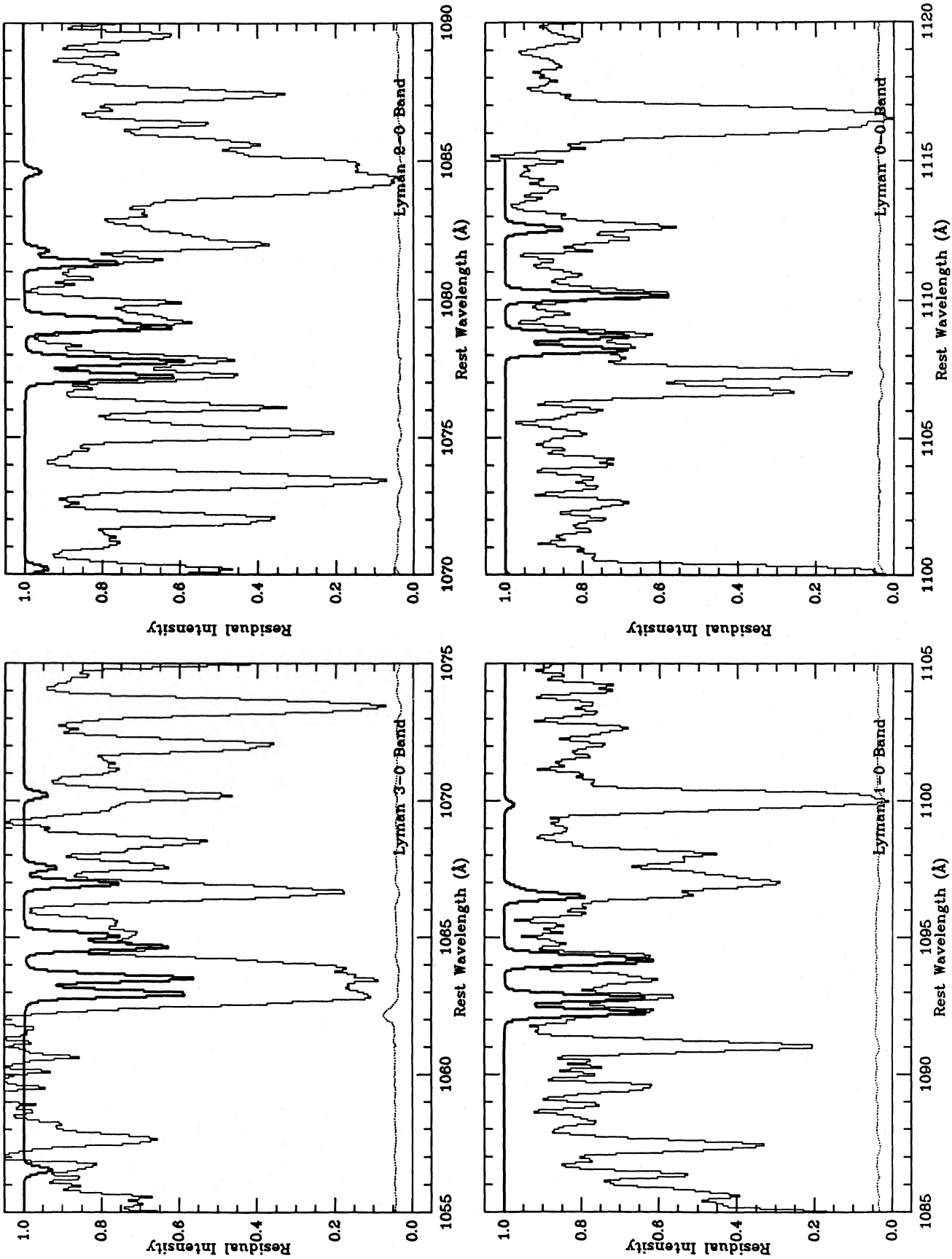


FIG. 4.—Expansion of the 1 Å resolution spectrum in the regions of strong expected H₂ absorption features. The synthetic spectrum with H₂ and atomic absorption is plotted in a heavy line. The Lyman 6-0 band is not shown since it is inexorably blended with atomic Ly β absorption. The strongest anticoincidence is near 932.5 Å, a region of low S/N and uncertain continuum placement.

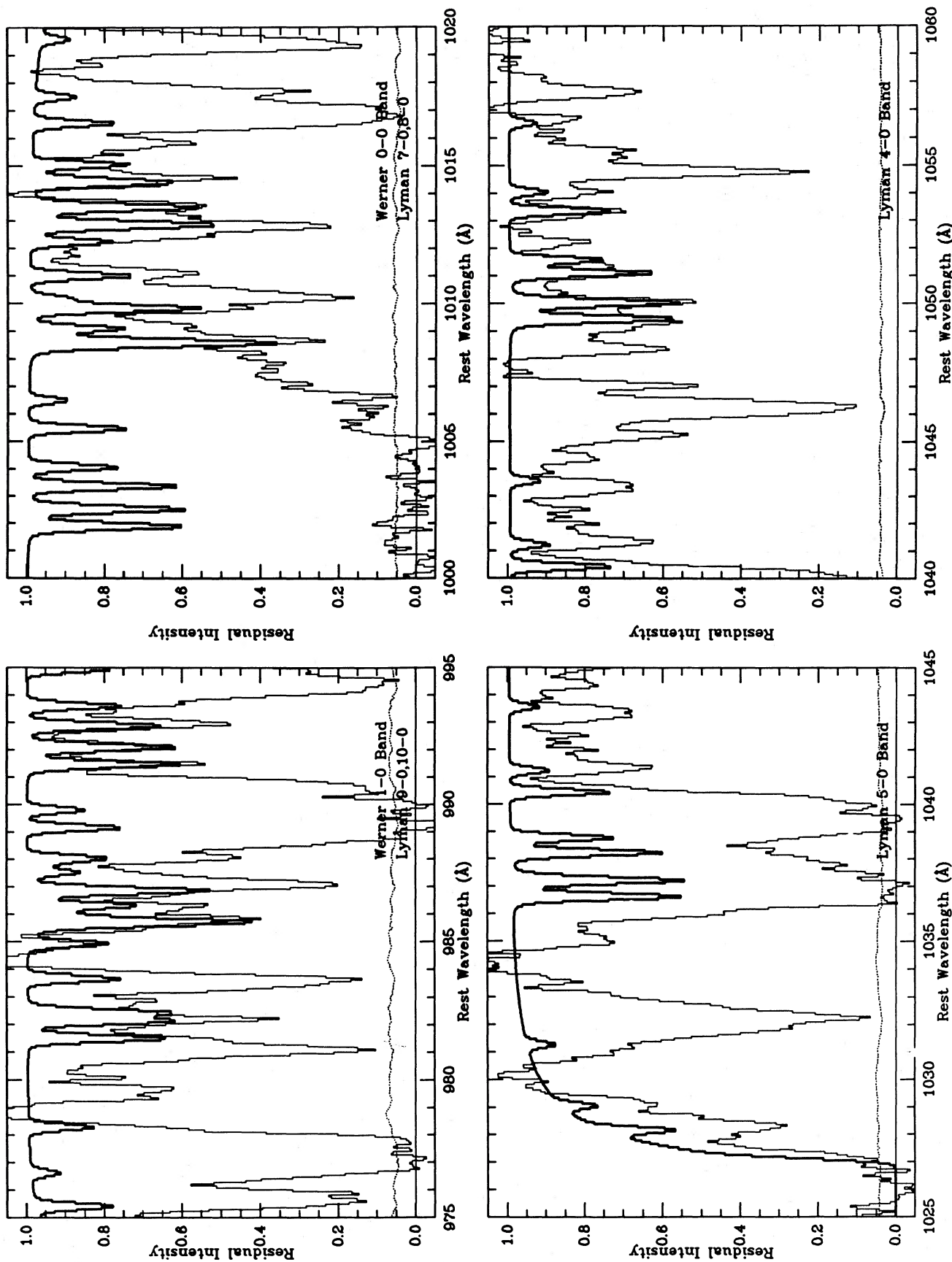


FIG. 4—(continued)

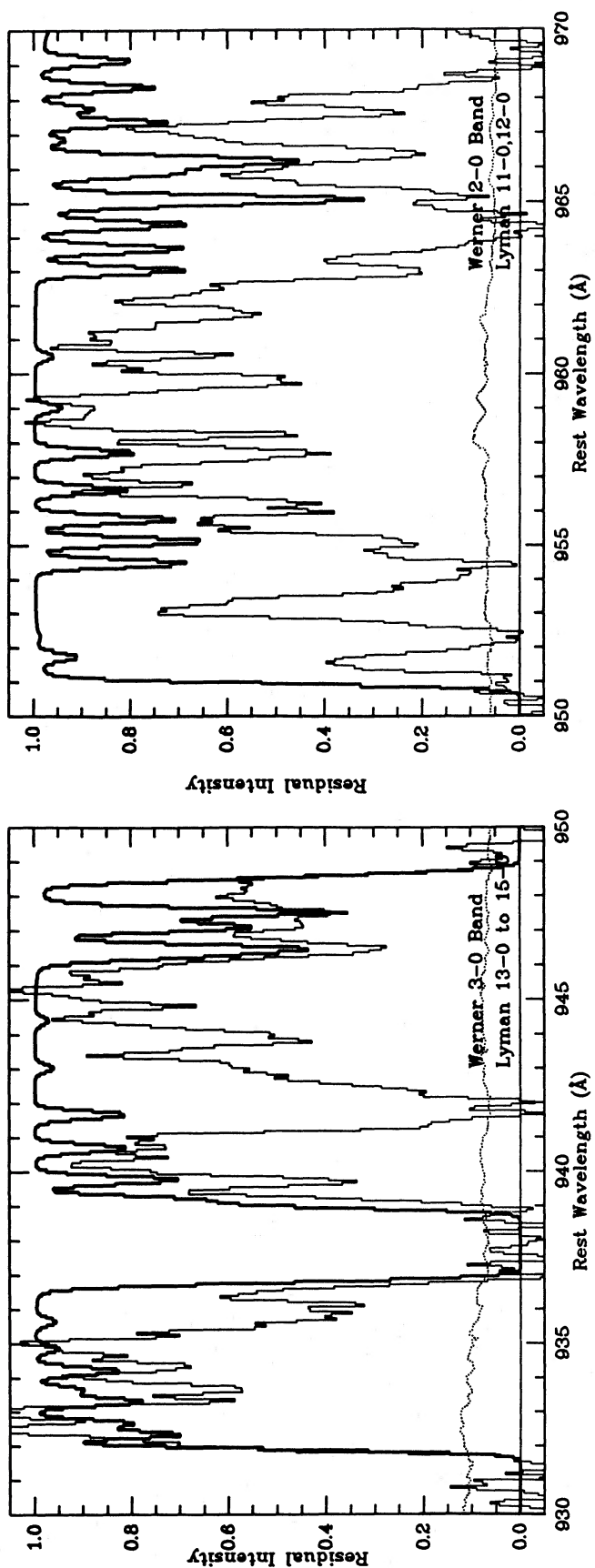


FIG. 4—(continued)

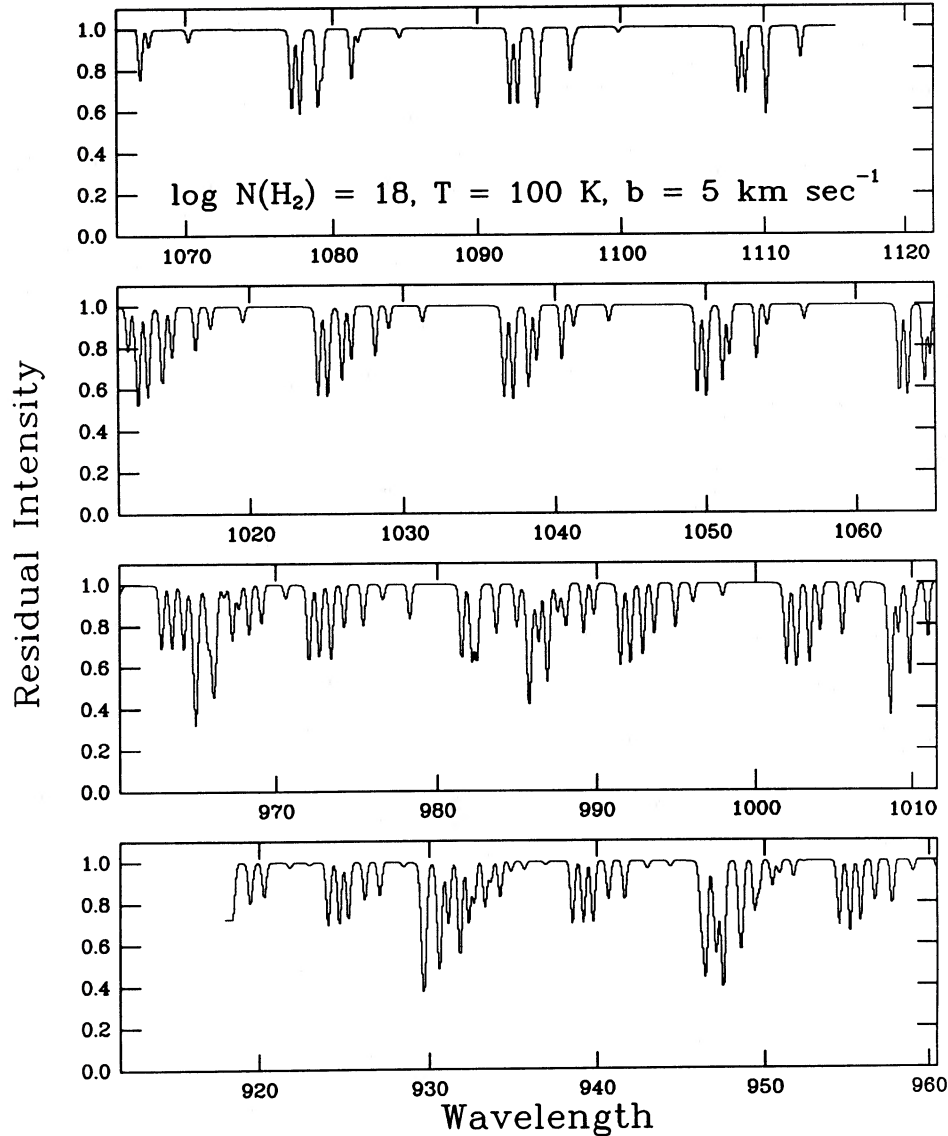


FIG. 5a

FIG. 5.—(a) Synthetic H_2 spectrum plotted on a logarithmic wavelength scale. (b) Normalized 1 \AA resolution data shifted to the restframe of the $z = 2.8110$ absorption line system and plotted on the same scale as panel (a). This panel can be photocopied onto a transparency and overlain on panel (a). By shifting the two figures parallel to the wavelength scale (corresponding to a shift in z) one can see that for most shifts, many anticoincidences between the real and synthetic spectra are found while few are found for zero shift.

in the fitting procedure is the establishment of the continuum. Errors in the continuum placement may result in errors in the measured equivalent widths of the weak features of more than a factor of 2. (2) There is no compelling reason to expect that the H_2 excitation can be characterized by a single value of the temperature. We did, however, perform some limited exploration of parameter space to try to understand what limits could be set on the physical conditions in the absorbing cloud. Based on these experiments, the following general comments can be made: At high temperature ($T_{\text{ex}} \geq 1000 \text{ K}$) and large Doppler parameter ($b = 25 \text{ km s}^{-1}$), we can rule out cases with $\log N(H_2) \geq 15.5$. If b is dropped to 10 km s^{-1} , $\log N(H_2)$ can be as high as 16 before a prohibitive number of anticoincidences result. At 100 K and $b = 25$, the data are consistent with $\log N(H_2) \approx 15$, however the lines of the Lyman 0–0, 1–0, and 2–0 bands are too weak to account for the observed features at the

appropriate wavelengths. In order to increase the strength of the predicted features in these bands relative to higher bands, we decreased the Doppler parameter in the syntheses resulting in increased saturation of the higher bands relative to the lower and a larger value of $N(H_2)$. We judge the fit to be tolerable for the set of conditions shown in the figures, that is, $\log N(H_2) = 18$, $T_{\text{ex}} = 100 \text{ K}$, and $b = 5 \text{ km s}^{-1}$.

The strategy used to derive these parameters was to determine the maximum column density for a given Doppler parameter and rotational population distribution. In that we cannot be sure of the identifications of the features we attribute to H_2 absorption due to the high probability of confusion by Ly α forest lines, our estimate of $\log N(H_2)$ is an upper limit for a low value of b . The apparent disparity between our results and those of Levshakov and Varshalovich [1985; $\log N(H_2) = 16.5$] is due to the large Doppler parameter ($\sim 100 \text{ km s}^{-1}$),

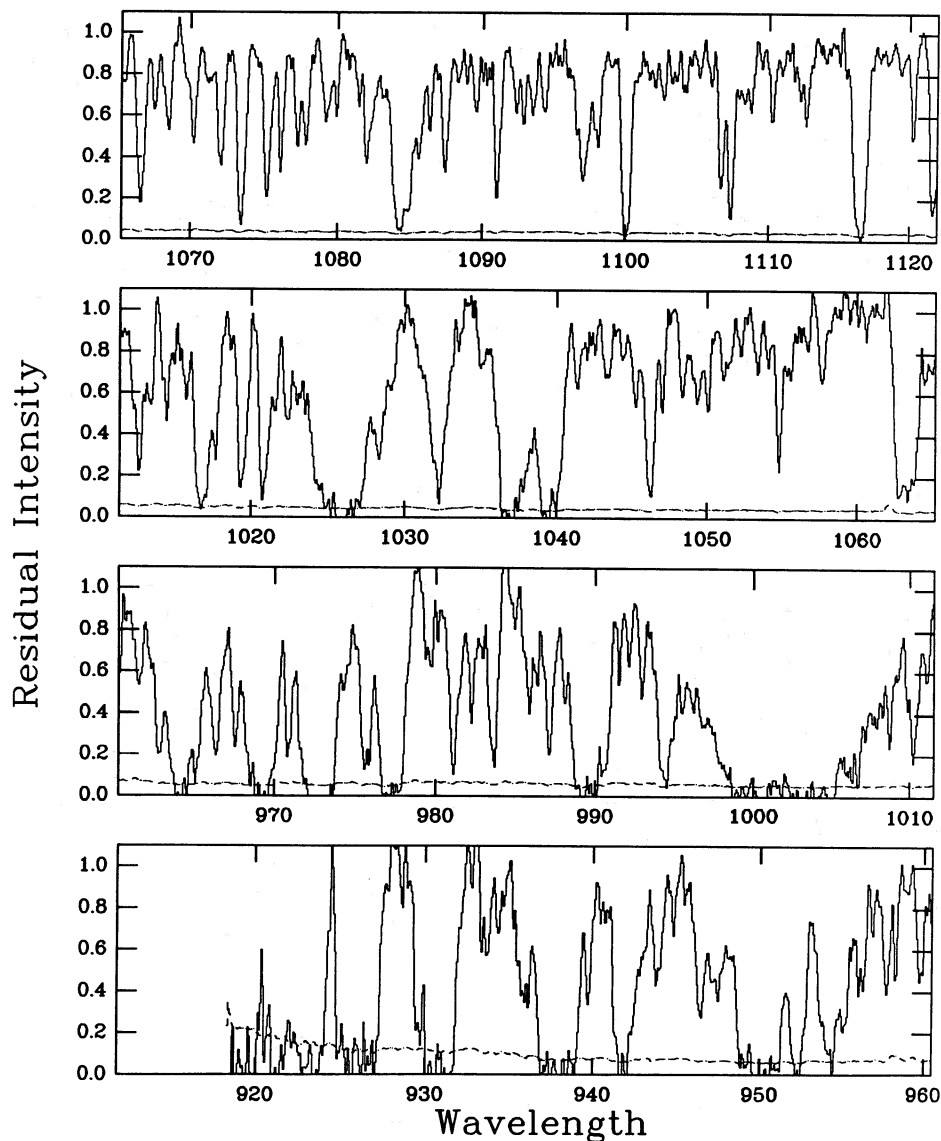


FIG. 5b

derived from a curve-of-growth analysis of O I, Si II, S II, and Fe II lines, used in their study. Given the presence of structure on small velocity scales, we consider a b -value derived from a curve of growth using 2 \AA resolution data to be unreliable.

IV. DISCUSSION

a) Implications Regarding the Absorbing Region

In the following discussion it is assumed that the identification of H_2 at $z = 2.8110$ is real and that the molecular absorbing region is characterized by $\log N(\text{H}_2) = 18 \text{ cm}^{-2}$, $T_{\text{ex}} = 100 \text{ K}$, and $b = 5 \text{ km s}^{-1}$. In Galactic clouds that contain this much H_2 it is usually thought that T_{ex} for the lowest levels ($J \leq 3$) is approximately equal to the kinetic temperature of the gas (see, e.g., Spitzer and Jenkins 1975) although more detailed analyses seem to require temperature gradients (van Dishoeck and Black 1986). Because the Doppler parameters inferred for H and H_2 , $b_{\text{H}} = 100 \gg b_{\text{H}_2} = 5 \text{ km s}^{-1}$, differ by a large factor, it is likely that the atomic hydrogen is more broadly distrib-

uted in space. The apparent molecular fraction, $f = 2 \times 10^{-3}$, should be regarded as a lower limit to the actual molecular fraction in the absorbing region. If this region were like the Galactic diffuse clouds surveyed by Savage *et al.* (1977), then $f \geq 2 \times 10^{-3}$ would correspond to $N_{\text{H}} \geq 5 \times 10^{20} \text{ cm}^{-2}$ and a visual extinction $A_V \geq 0.3 \text{ mag}$ on average. There are, however, some Galactic clouds in this sample in which the extinction seems to be near zero while $N(\text{H}_2) > 10^{19} \text{ cm}^{-2}$. For a typical Galactic value of the gas/extinction ratio, $N_{\text{H}}/A_V \approx 1.59 \times 10^{21} \text{ cm}^{-2} \text{ mag}^{-1}$, the total neutral column density would be expected to be accompanied by an extinction $A_V \approx 0.8 \text{ mag}$. As pointed out previously by Smith, Jura, and Margon (1979), there is no evidence for any extinction. Additional photometry extending out to $\lambda = 5800 \text{ \AA}$ in the $z = 2.811$ rest frame (Soifer *et al.* 1983) indicates that the intrinsic flux distribution of PKS 0528–250 would be exceedingly peculiar if even as much as $A_V = 0.3 \text{ mag}$ of extinction were present.

The molecular fraction at $z = 2.811$ toward PKS 0528–250 is ~ 1000 times larger than the limit, $f < 4 \times 10^{-6}$, established

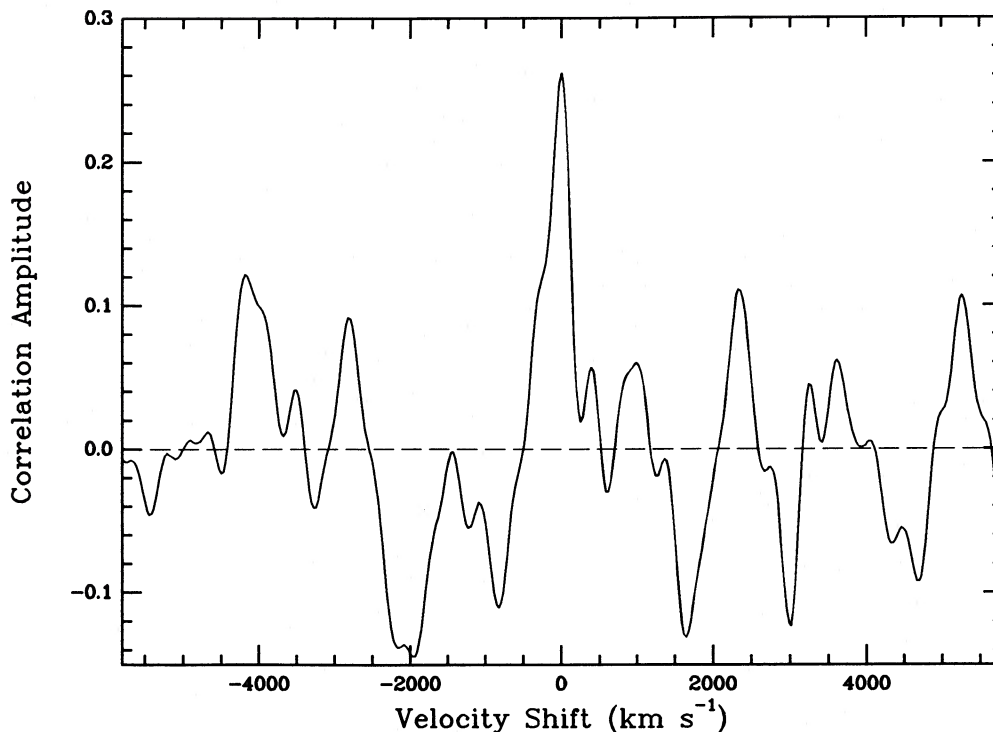


FIG. 6.—Cross correlation of the two spectra shown in Fig. 4. The peak near zero velocity has the largest amplitude by more than a factor of 2 of any peak in the range $-10,000$ to $+10,000$ km s^{-1} . Regions around atomic Lyman lines were excised from the observed spectrum prior to performing the cross correlation.

TABLE 2
POSSIBLE H_2 ABSORPTION FEATURES

Line	λ_{syn}	λ_{obs}^a	Z_{obs}	Identification ^b
1.....	946.43	3607.03	2.81120	W3-0 R(0) + R(1)
2.....	947.47	3610.71	2.81090	W3-0 Q(1) + L14-0 P(1)
3.....	984.94	3753.26	2.81065	L10-0 P(2)
4.....	985.73	3756.67	2.81105	W1-0 R(0) + R(1) ^c
5.....	991.47	3778.37	2.81088	L9-0 R(0)
6.....	992.07	3780.76	2.81098	L9-0 R(1)
7.....	1008.59	3843.71	2.81097	W0-0 R(0) + R(1) ^d
8.....	1009.86	3848.34	2.81077	W0-0 Q(1)
9.....	1012.86	3859.62	2.81062	L7-0 R(0) ^e
10.....	1013.50	3862.37	2.81092	L7-0 R(1)
11.....	1015.03	3868.10	2.81082	L7-0 R(2) + W0-0 Q(4) ^f
12.....	1049.46	3998.92	2.81045	L4-0 R(0)
13.....	1050.00	4001.53	2.81098	L4-0 R(1)
14.....	1051.14	4005.43	2.81056	L4-0 P(1)
15.....	1051.55	4007.03	2.81059	L4-0 R(2)
16.....	1053.34	4014.04	2.81077	L4-0 P(2)
17.....	1064.71	4057.10	2.81052	L3-0 P(1)
18.....	1077.24	4105.15	2.81080	L2-0 R(0)
19.....	1077.76	4107.32	2.81098	L2-0 R(1)
20.....	1081.33	4121.28	2.81131	L2-0 P(2)
21.....	1092.27	4162.77	2.81112	L1-0 R(0)
22.....	1092.77	4164.48	2.81094	L1-0 R(1)
23.....	1094.19	4169.99	2.81103	L1-0 P(1)
24.....	1108.70	4225.06	2.81082	L0-0 R(1)
25.....	1110.12	4230.50	2.81085	L0-0 P(1)
26.....	1112.56	4239.93	2.81097	L0-0 P(2) + R(3)

^a Wavelengths are heliocentric, vacuum values.

^b L denotes Lyman bands; W, Werner bands.

^c Possibly blended with CO J-X(0, 0).

^d Possibly blended with Cl III $\lambda 1008.777$ at $z = 2.8103$.

^e Possibly blended with S III $\lambda 1012.504$ at $z = 2.8120$.

^f Possibly blended with Cl III $\lambda 1015.023$ at $z = 2.8108$.

for the $z = 2.309$ system toward PHL 957 (Paper II). This difference must result from a more efficient H_2 formation rate or a much reduced H_2 dissociation rate or both, in the PKS 0528 – 250 absorbing cloud if the molecular abundance is in steady state. The absence of any obvious extinction suggests that the surface area in dust particles may be too small to maintain a large formation rate. Further analysis of atomic line data will be required to determine whether the ultraviolet radiation field incident on the $z = 2.811$ molecular cloud is sufficiently weak to permit the existence of the inferred molecular fraction. An alternative explanation is the nonequilibrium formation of H_2 in the cooling zones behind shocks such as those described by MacLow and Shull (1986).

b) Limits on Variations of the Electron to Proton Inertial Mass Ratio

The potential diagnostic applications of the observation of molecules at high redshift are many; however, the extreme line blending and modest spectral resolution of the data presented here as well as the even lower resolution spectra of the metal lines in this system make the existing data less than adequate for detailed study of the cloud properties. If we take the identification of H_2 at face value, however, one observable which is of interest and can be fairly tightly constrained is the identity of the redshift of lines from various bands within the Lyman band system.

Thompson (1975) pointed out that since the wavelengths of molecular transitions are sensitive to the ratio of electron to proton inertial mass, observations of molecular transitions at large look-back times can provide a check on the invariance of this ratio with cosmic time. In the case of H_2 , if the ratio m_e/m_p in the absorber differs from the present value, then the pattern of molecular absorption lines would not be well fitted with a

single value of the redshift. In particular, the 0–0 band of the system would have essentially the same redshift as the atomic lines arising in the same gas cloud while higher bands would have redshifts which differ from the atomic lines by a progressively larger amount as the vibrational component of the energy increases with the increasing vibrational quantum numbers of the upper state.

The most conservative constraint on the invariance of the m_e/m_p ratio is provided by the near identity of the redshifts of the features attributed to the Lyman 10–0 $P(2)$ and 2–0 $P(2)$ lines. The data imply an upper limit on the fractional variation of 2.0×10^{-4} in the mass ratio from $z = 2.811$ to $z = 0$, based on the energy levels and Dunham coefficients for the $B^1\Sigma_u^+$ state of H_2 of Dabrowski (1984).

c) Suggestions for Further Study

We have presented data which *strongly suggest* that a substantial column density of H_2 exists in the $z = 2.811$ absorption system toward PKS 0528–250. Additional confirmatory evidence could be provided by high S/N observations at higher resolution, yielding more accurate wavelengths of the putative molecular features and perhaps a more accurate determination of the continuum placement. Furthermore, such data would be of interest in understanding the physical conditions in the material responsible for the redshift component containing the H_2 . The best published data on the low ionization lines at $z = 2.811$ have a spectral resolution of only 2 \AA , insufficient to provide details of substructure in the absorption lines at less-

than the 100 km s^{-1} level. Also, recent unpublished studies (Meyer, private communication) show that the heavy element abundances in the absorber may be quite high and may have a solar Ni abundance so a detailed abundance analysis from such data may yield very interesting results.

Although PKS 0528–250 is a strong radio source ($S_{6\text{cm}} = 1.13 \text{ Jy}$; Veron-Cetty and Veron 1985), it is not known if this system contains 21 cm absorption as does the system in MC 1331+170. Observations at redshifted 21 cm may clarify the distribution of neutral hydrogen on small velocity scales. Furthermore, detection of 21 cm absorption may allow an estimate of the column density of H I and the H I spin temperature in the subcomponent responsible for the molecular hydrogen absorption and thereby allow direct comparison of the ratio $2N(H_2)/N(H \text{ I})$ with that in the interstellar medium of the Galaxy.

We thank Ruth Peterson for performing the cross-correlation analysis for us and for interesting discussions. We have profited from conversations and encouragement from David Meyer, Ray Weymann, Rodger Thompson, Simon Morris, and John Stocke. We are particularly grateful for correspondences from Sergei Levshakov, whose diligent searches for molecular hydrogen absorption stimulated this work. This study was supported in part by a grant from the Scholarly Studies Program of the Smithsonian Institution and by the NSF through grants AST 84-03766 and 87-00741.

REFERENCES

- Black, J. H., Chaffee, F. H., Jr., and Foltz, C. B. 1987, *Ap. J.*, **317**, 442 (Paper II).
 Chaffee, F. H., Jr., and Latham, D. W. 1982, *Pub. A.S.P.*, **94**, 386.
 Chaffee, F. H., Jr., Foltz, C. B., and Black, J. H. 1986, *Pis'ma Astr. Zh.*, **12**, 819 (Paper I. English trans. in *Soviet Astr. Letters*, in press.)
 ———, 1988, in preparation (Paper III).
 Chen, J., and Morton, D. C. 1984, *M.N.R.A.S.*, **208**, 167.
 Dabrowski, I. 1984, *Canadian J. Phys.*, **62**, 1639.
 Gaskell, C. M. 1982, *Ap. J.*, **263**, 79.
 Levshakov, S. A., and Varshalovich, D. A. 1985, *M.N.R.A.S.*, **212**, 517.
 MacLow, M.-M., and Shull, J. M. 1986, *Ap. J.*, **302**, 585.
 Morton, D. C., Chen, J., Wright, A. E., Peterson, B. A., and Jauncey, D. L. 1980, *M.N.R.A.S.*, **193**, 399.
 Oke, J. B. 1974, *Ap. J. Suppl.*, **27**, 21.
 Savage, B. D., Bohlin, R. C., Drake, J. F., and Budich, W. 1977, *Ap. J.*, **216**, 291.
 Smith, H. E., Jura, M., and Margon, B. 1979, *Ap. J.*, **228**, 369.
 Soifer, B. T., Neugebauer, G., Oke, J. B., Matthews, K., and Lacy, J. H. 1983, *Ap. J.*, **265**, 18.
 Spitzer, L., Jr., and Jenkins, E. B. 1975, *Ann. Rev. Astr. Ap.*, **13**, 133.
 Thompson, R. I. 1975, *Ap. Letters*, **16**, 3.
 Tonry, J., and Davis, M. 1979, *A. J.*, **84**, 1511.
 van Dishoeck, E. F., and Black, J. H. 1986, *Ap. J. Suppl.*, **62**, 109.
 Veron-Cetty, M.-P., and Veron, P. 1985, *ESO Sci. Rep.*, No. 4.
 Wilkes, B. J., and Carswell, R. F. 1982, *M.N.R.A.S.*, **201**, 645.
 Wolfe, A. M., Turnshek, D. A., Smith, H. E., and Cohen, R. D. 1986, *Ap. J. Suppl.*, **61**, 249.

JOHN H. BLACK: Steward Observatory, University of Arizona, Tucson, AZ 85721.

FREDERIC H. CHAFFEE, JR., and CRAIG B. FOLTZ: Multiple Mirror Telescope Observatory, University of Arizona, Tucson, AZ 85721-0465